33RD INTERNATIONAL COSMIC RAY CONFERENCE, RIO DE JANEIRO 2013
THE ASTROPARTICLE PHYSICS CONFERENCE

ICRC 2013

The Energy Scale of the Pierre Auger Observatory

VALERIO VERZI[1] FOR THE PIERRE AUGER COLLABORATION[2]

[1] *INFN, Sezione di Roma "Tor Vergata", via della Ricerca Scientifica 1, 00133 Roma, Italia*
[2] *Full author list: http://www.auger.org/archive/authors_2013_05.html*

auger_spokespersons@fnal.gov

Abstract: The energy scale of the Pierre Auger Observatory is derived from fluorescence observations of extensive air showers, an intrinsically calorimetric technique. Taking advantage of more precise measurements of the fluorescence yield, of a deeper understanding of the detector and consequently improved event reconstruction and of a better estimate of the *invisible energy*, we present an update of the method used to determine the energy scale. Differences in energy with respect to earlier measurements and the systematic uncertainties associated with the new energy scale are discussed.

Keywords: Pierre Auger Observatory, ultra-high energy cosmic rays, energy spectrum, energy scale.

1 Introduction

The Pierre Auger Observatory [1] has been designed to study ultra-high energy cosmic rays with unprecedented statistics and with low systematic uncertainties. It comprises an array of 1660 water-Cherenkov detectors deployed over 3000 km^2, collectively called the surface detector array (SD) with the atmosphere above it viewed by the Fluorescence Detector (FD) [2]. The FD consists of 27 telescopes located at 5 sites on the periphery of the SD array. Each telescope contains 440 photomultiplier pixels that detect light focused by a large spherical mirror.

The *hybrid* combination of the FD and the SD has an enormous advantage in the determination of the energy scale. The FD provides a nearly calorimetric energy measurement as the fluorescence light is produced in proportion to the energy dissipation by a shower in the atmosphere. These measurements are performed with a duty cycle of about 13%, as the FD can only operate during clear nights with little moonlight. The SD measures the distribution of particles on the ground with a duty cycle of almost 100%. By means of showers viewed by the FD in coincidence with the SD (*hybrid* events), the signal detected by the SD at 1000 m from the shower axis is calibrated against the calorimetric energy measured with the FD [3]. The advantage of the hybrid detector is therefore that the energy assignment is largely independent of air shower simulations.

The reconstruction of the fluorescence events is a complex process that requires the knowledge of several parameters. The FD measures the number of fluorescence photons produced from the de-excitation of atmospheric nitrogen molecules excited by the charged particles of the shower. The emission of these photons is isotropic and mostly in the wavelength range between 300 and 430 nm. The fluorescence yield is the proportionality factor between the number of photons emitted and the energy deposited in the atmosphere. It is therefore a key ingredient for the reconstruction: the light collected by the FD telescopes as a function of the atmospheric depth X can be converted to the longitudinal profile of the energy deposit (dE/dX) of the air shower. An accurate reconstruction of dE/dX requires continuous monitoring of the atmospheric conditions. This is particularly important for estimating the attenuation of the light due to molecular and aerosol scattering as it travels from the shower to the telescopes. Another key ingredient is the absolute calibration of the telescopes. Finally, the integral $\int dE/dX dX$ represents essentially the electromagnetic energy of the shower. The total energy is obtained from the calorimetric energy by adding the so-called *invisible energy* which accounts for the energy carried into the ground by high energy muons and neutrinos.

Using new knowledge both at the level of the detector and of the fluorescence process, we have updated the reconstruction of fluorescence events. In sections 2-6 we describe the changes made to the different parts of the reconstruction chain. For each we address the effects on FD energy determination and related systematic uncertainties, distinguishing between correlated and non-correlated errors between different showers. This is crucial to correctly propagate the uncertainties from FD measurements to SD energies in the calibration of SD events, which is updated in section 7 where we discuss the differences with respect to the previous energy scale and we summarise the total uncertainty of the new determination of the energy.

2 The fluorescence yield

The parameters characterising the fluorescence yield include an absolute normalisation of the wavelength spectrum, the relative intensities in different spectral bands, and their dependencies on pressure, temperature and humidity.

Previously the Auger collaboration used all of the parameters measured in the Airfly experiment [4, 5] with the exception of the absolute normalisation of the spectrum. This is parameterised by the intensity of the 337 nm spectral band and in the past we used the measurement of Nagano et al. [6] which has an uncertainty of 14%. The uncertainty of the absolute yield made the largest contribution to the overall uncertainty of the energy scale (22%).

We have now adopted a precise measurement of the absolute yield of the 337 nm band made by the Airfly collaboration with an uncertainty of 4% [7]. The Airfly measurement is the most precise available and it is compatible with the analysis presented in [8]. Its impact in the reconstruction of FD events is very important. Shower energies are lowered by about 8% and the precision due to the uncertainty of the measurement of the absolute yield is on average 3.4%.

As the yield is now known with high precision, we have also evaluated the uncertainties arising from the other fluorescence parameters. These uncertainties have been calculated by changing the fluorescence parameters by their uncertainties according to their degree of correlation reported in the Airfly papers [4, 5]. The uncertainty in shower energies arising from the relative intensities of the bands of the fluorescence spectrum is 1%. Those arising from the pressure, temperature and humidity dependencies are respectively 0.1%, 0.3% and 0.1%.

3 The atmosphere

An extensive array of instruments were designed and are deployed to monitor the atmosphere at the Pierre Auger Observatory [9]. The aerosol monitoring uses two lasers placed near the center of the array, four elastic scattering lidar stations, two optical telescopes and two systems which monitor the differential angular distribution of the aerosol scattering cross section (the *phase function*). Four infra-red cameras are used for cloud detection.

We have improved the hourly estimates of the aerosol optical depth profile [10] used to calculate the aerosol transmission factor [11] . The uncertainty on these profiles has two components, one correlated and another uncorrelated between different showers, components giving rise to an uncertainty in the shower energies which increases with energy from 3% to 6%. Other correlated uncertainties related to aerosols are those from the measurements of the *phase function* and from the wavelength dependence of the scattering cross-section. They are 1% and 0.5% respectively. Another uncorrelated uncertainty of 1% is associated with the spatial variability of the aerosols across the site [9].

The density profiles of the atmosphere are estimated using the Global Data Assimilation System (GDAS) meteorological model [12]. The day-to-day fluctuations of the pressure, temperature and humidity around the GDAS model have been estimated using meteorological radio-sondes launched locally. From studies of these fluctuations, we have identified an uncorrelated uncertainty in the energies of about 1% and a correlated one of about 1%.

4 The absolute calibration of the telescopes

Periodically the FD telescopes are calibrated absolutely with a drum-shaped light source (*drum*) placed in front of the diaphragm [2]. In this way we perform an end-to-end calibration of all elements of the telescope. The absolute calibration is made at 375nm with an uncertainty of 9%. This is fully correlated between different showers. Following the progress reported in [13], the Collaboration is working to reduce this uncertainty to the 5% level.

The short and long term changes of the detector response are tracked by a relative optical calibration system [2]. The response of the photomultipliers (PMTs) to the relative calibration performed during the *drum* operation and before and after each night of data taking are used to track the absolute calibration in the periods between the *drum* measurements. Two uncertainties are associated with this tracking, 3% for the uncorrelated part and 2% for the correlated one.

A new feature of the event reconstruction is the treatment of the calibration constants of the pixels. The optical properties of the telescopes have been studied using an isotropic point-like source put in the field of view of a telescope using a flying platform [14]. For a fixed position of the light source, we have discovered that the reflectivity of the PMT surface causes an optical *halo* extending over the full focal surface of the telescope. The *drum* calibration constants have been corrected for this effect with shower energy increasing by about 3%.

A further improvement concerns the relative FD response at various wavelengths. We have introduced a more precise optical efficiency curve measured using the *drum* device while in the past we used the optical efficiencies of the each component of the telescopes. This revised efficiency increases the shower energies by about 4%. The uncertainty in the measurement propagated to the shower energies introduces a correlated uncertainty of 3.5%.

5 Reconstruction of the longitudinal profile of the showers

A further change in the event reconstruction is due to an improved technique for the determination of the energy deposit in atmosphere [2, 15]. In a FD telescope a shower is observed as a sequence of pixels triggered at different times. The pointing direction of the pixels and FD and SD timing information are used to determine the position of the shower axis in the sky. The longitudinal profile of the light is derived from the time traces of the PMTs. The pixel selection is made by maximising the signal-to-noise ratio, excluding the night-sky light that dominates off the image axis. Knowing the shower geometry, the FD absolute calibration, the attenuation of the light flux in the atmosphere and by estimating the number of Cherenkov photons detected by the FD, it is possible to calculate the energy deposit with a fit to the dE/dX data being made using Gaisser-Hillas [16] function. This enables an estimate of the energy deposit even outside the field of view of the telescopes and therefore yields the energy deposited in the atmosphere.

Because of the intrinsic shower width and the optical point spread function of the telescopes, part of the incoming light is spread away from the image axis, in the field of view of the non-selected pixels. The contribution of this light to the dE/dX is calculated by estimating the size of the shower image at the telescope diaphragm. Two models are used for the fluorescence [17] and Cherenkov [18] light. We have now introduced a further correction which takes into account the angular spread close to the shower axis produced by the optical elements of the FD telescope [14]. The folding of this point spread function with the intrinsic shower width spreads the light more than predicted by the two models that only take into account the shower width. This effect has been parameterised by analysing shower data and it increases the shower energy by an amount ranging from 5% to 9% (the correction is larger at lower energies). We assign, conservatively, a correlated systematic uncertainty in the light collection of about 5%.

A further complication arises from the light which reaches the telescopes after multiple scatterings in the atmosphere. To avoid an overestimation of the shower energy, this light must be subtracted from the profile of detected photons. The multiple scattering contribution has been parameterised using [19] and the uncertainty of it affects the shower energies in a fully correlated way by about 1% [9].

In a further update we have developed a maximum likelihood fit taking into account realistic fluctuations of the

signal in the PMTs. This increases the shower energies by about 2%.

To improve the fit of dE/dX, a Gaussian constraint is imposed on the parameters that define the Gaisser-Hillas function [15]. Changing these constraints by one standard deviation, we have evaluated a further correlated uncertainty in the shower energy which ranges from 3.5% to 1% (it decreases with energy). Other errors on the energies arise from the statistical error of the dE/dX fit which decreases with energy from 5% to 3%, and an average uncertainty of 1.5% that arises from the uncertainty in the shower axis geometry. Both effects are uncorrelated.

The full reconstruction technique has been tested using Monte Carlo simulations. On average, the reconstructed energies differ from the true ones by about 2%. This bias has been considered as another correlated uncertainty.

6 The invisible energy

The final update in the reconstruction concerns the estimate of the *invisible energy* [20]. Previously we used an estimate based entirely on simulated showers [21] while now it is derived from data. This significantly reduces the dependence on the hadronic interaction models and mass composition. The *invisible energy* (E_{inv}) can be calculated for each shower using the FD measurement of the longitudinal profile and the SD signal at 1000 m from the axis, $S(1000)$. E_{inv} can be reliably estimated only above 3×10^{18} eV (the energy above which the SD array is fully efficient) as below this energy $S(1000)$ is biased by upward fluctuations of the shower signals. As the FD detects showers at lower energies and since we want to update the *invisible energy* for all FD events, E_{inv} is parameterised with an analytical function above 3×10^{18} eV, with the function being extrapolated to 10^{17} eV.

The same set of hybrid showers used to calibrate the SD energies (see below) is used to find the relation between E_{inv} and the calorimetric energy E_{cal}: $E_{inv} = a_0(E_{cal}[\mathrm{EeV}])^{a_1}$. The fit is performed by minimising a χ^2 function which takes into account the fluctuations of both FD and SD measurements, yielding the parameters: $a_0 = (0.174\pm0.001)\times10^{18}$ eV and $a_1 = 0.914\pm0.008$. The correlation coefficient of the two parameters is -1.

The number of muons measured with the SD [22] is higher than predicted by the simulations formerly used to derive the *invisible energy* [21]. This contribution to the primary energy now ranges between 15% at 10^{18} eV and 11% at the highest energies (before we had $11\%\div8\%$) with total shower energies increasing by about 4%. Analysis of the systematic uncertainties on the *invisible energy* [20] shows a correlated uncertainty in the total energy which decreases with energy from 3% to 1.5%. With the old parameterisation the overall uncertainty was 4%.

Due to the stochastic nature of air showers, the *invisible energy* is also affected by shower-to-shower fluctuations. These are parameterised according to [15] and an uncorrelated uncertainty of about 1.5% is introduced.

7 Impact on the energy scale and on its systematic uncertainty

The changes in the event reconstruction described in the previous sections have an impact on the energy determination and associated uncertainty for both FD and SD events. Concerning FD energies, all changes are summarised in table 1, for a reference energy of 10^{18} eV. Figure 1 shows the cumulative energy shift as a function of the shower energy when we introduce the effects described in sections 2, 4, 5 and 6. The update of the analysis of the aerosol optical depth profiles described in section 3 does not change the shower energies significantly. The overall change ranges from about +16% at 10^{18} eV to +12% at 10^{19} eV . We note that the new energy scale is consistent with the old one for which we gave an overall systematic uncertainty of 22% [3]. Moreover the changes are also consistent within each sector of the reconstruction. Indeed in [3] we quoted uncertainties of 14% for the fluorescence yield, 9.5% for the FD calibration, 10% for the longitudinal profile reconstruction and 4% for the *invisible energy*.

Changes in FD energies at 10^{18} eV	
Absolute fluorescence yield (sec. 2)	**-8.2%**
New optical efficiency	4.3%
Calibr. database update	3.5%
Sub total (FD calibration - sec. 4)	**7.8%**
Likelihood fit of the profile	2.2%
Folding with the point spread function	9.4%
Sub total (FD profile reconstruc. - sec. 5)	**11.6%**
New invisible energy (sec. 6)	**4.4%**
Total	**15.6%**

Table 1: Changes to the energy of showers at 10^{18} eV.

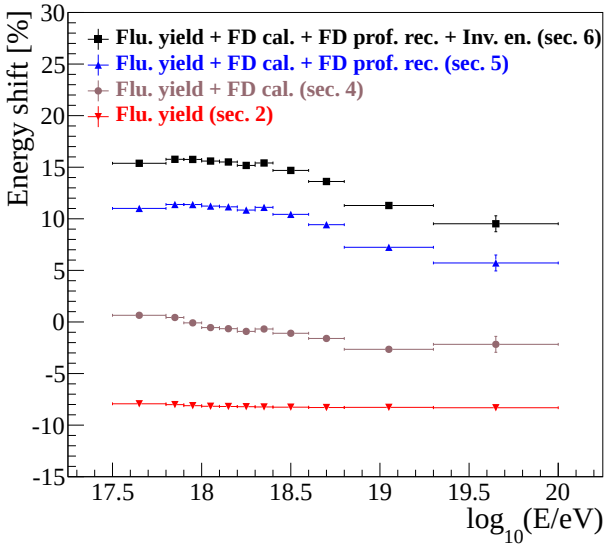

Figure 1: Cumulative energy shift as a function of the shower energy when we introduce the various effects.

The SD energies are obtained on the basis of the analysis presented in [3] with the new selection criteria described in [23]. The SD energy estimator, S_{38}, may be regarded as the signal $S(1000)$ that the shower would have produced had it arrived with a zenith angle, $\theta = 38^\circ$.The relation between S_{38} and the FD energy E_{FD} is well described by a single power-law function, $E_{FD} = AS_{38}^B$. The parameters have been updated with a fit to a subset of high-quality hybrid events with $\theta < 60^\circ$ detected between 1 January 2004 and 31

December 2012. The number of showers above 3×10^{18} eV is 1475. The fit takes into account the resolutions of both E_{FD} and S_{38} (see table 2). The resolution of E_{FD} is determined using all uncorrelated uncertainties described above. The fit yields: $A = (0.190 \pm 0.005) \times 10^{18}$ eV and $B = 1.025 \pm 0.007$ and with a correlation coefficient of -0.98. The root-mean-square deviation of the distribution of AS_{38}^B/E_{FD} is about 18.5%. It is dominated by low-energy showers and is compatible with the expected resolution obtained from the quadratic sum of all the uncertainties listed in table 2 (18% at 3×10^{18} eV).

Uncertainties entering into the SD calibration fit	
Aerosol optical depth	3%÷6%
Horizontal uniformity	1%
Atmosphere variability	1%
Nightly relative calibration	3%
Statistical error of the profile fit	5%÷3%
Uncertainty in shower geometry	1.5%
Invis. energy (shower-to-shower fluc.)	1.5%
Sub total FD energy resolution	**7% ÷ 8%**
Statistical error of the $S(1000)$ fit [3]	12% ÷ 3%
Uncert. in lateral distrib. function [3]	5%
shower-to-shower fluctuations [3]	10%
Sub total SD energy resolution	**17% ÷ 12%**

Table 2: Uncertainties uncorrelated between different showers and affecting the SD energy estimator.

The large number of hybrid showers detected over 9 years has allowed several consistency checks [24]. The SD energy estimator ($E_{SD} = AS_{38}^B$ for a given value of S_{38}) has been studied by making calibration fits to data collected during different time periods and/or under different conditions. We have found that E_{SD} is stable within 5%, significantly above the statistical uncertainties. Even though these variations of E_{SD} are consistent with the quoted systematic uncertainties, we use them conservatively to introduce another uncertainty of 5%.

The FD uncertainties correlated between different showers should be propagated to the SD energy scale by shifting all FD energies coherently by their uncertainties. This means that the correlated uncertainties propagate entirely to the SD energies. Table 3 lists all uncertainties on the Auger energy scale. Most of them have a mild dependence on energy. When this dependence is non-negligible, we report the variation of the uncertainty in the energy range between 3×10^{18} eV and 10^{20} eV. The total uncertainty is about 14% and approximately independent of energy. We stress that we have made a significant improvement by comparison with the total 22% uncertainty reported previously [3].

Systematic uncertainties on the energy scale	
Absolute fluorescence yield	3.4%
Fluor. spectrum and quenching param.	1.1%
Sub total (Fluorescence yield - sec. 2)	**3.6%**
Aerosol optical depth	3%÷6%
Aerosol phase function	1%
Wavelength depend. of aerosol scatt.	0.5%
Atmospheric density profile	1%
Sub total (Atmosphere - sec. 3)	**3.4%÷6.2%**
Absolute FD calibration	9%
Nightly relative calibration	2%
Optical efficiency	3.5%
Sub total (FD calibration - sec. 4)	**9.9%**
Folding with point spread function	5%
Multiple scattering model	1%
Simulation bias	2%
Constraints in the Gaisser-Hillas fit	3.5% ÷ 1%
Sub total (FD profile rec. - sec. 5)	**6.5% ÷5.6%**
Invisible energy (sec. 6)	**3%÷1.5%**
Stat. error of the SD calib. fit (sec. 7)	**0.7%÷1.8%**
Stability of the energy scale (sec. 7)	**5%**
Total	**14%**

Table 3: Systematic uncertainties on the energy scale.

References

[1] The Pierre Auger Collaboration, Nucl. Instrum. Meth. A **523** (2004) 50.
[2] The Pierre Auger Collaboration, Nucl. Instrum. Meth. A **620** (2010) 227.
[3] R. Pesce, for the Pierre Auger Collaboration, Proc. 32nd ICRC, Beijing, China, 2 (2011) **214**, arXiv:1107.4809.
[4] M. Ave et al., Nucl. Instrum. Meth. A **597** (2008) 50.
[5] M. Ave et al., Astropart. Phys. **28** (2007) 41.
[6] M. Nagano et al., Astropart. Phys. **22** (2004) 235.
[7] M. Ave et al., Astropart. Phys. **42** (2013) 90.
[8] J. Rosado and F. Arqueros, paper 377, these proceedings.
[9] The Pierre Auger collaboration, Astropart. Phys. **33** (2010) 108.
[10] L. Valore, for the Pierre Auger Collaboration, paper 920, these proceedings.
[11] The Pierre Auger collaboration, JINST **8** (2013) 4009.
[12] The Pierre Auger collaboration, Astropart. Phys. **35** (2012) 591.
[13] J. T. Brack et al., JINST **8** (2013) 5014.
[14] J. Baeuml, for the Pierre Auger Collaboration, paper 806, these proceedings.
[15] M. Unger et al., Nucl. Instrum. Meth. A **588** (2008) 433.
[16] T. K. Gaisser, A. M. Hillas, Proc. 15th ICRC **8** (1977) 353.
[17] D. Gora et al., Astropart. Phys. **22** (2004) 29.
[18] M. Giller and G. Wieczorek, Astropart. Phys. **31** (2009) 212.
[19] M. D. Roberts, J. Phys. G Nucl. Partic. **31** (2005) 1291.
[20] M. Tueros, for the Pierre Auger Collaboration, paper 705, these proceedings.
[21] H. M. J. Barbosa et al., Astropart. Phys. **22** (2004) 159.
[22] I. Valino, for the Pierre Auger Collaboration, paper 635, these proceedings.
[23] D. Ravignani, for the Pierre Auger Collaboration, paper 693, these proceedings.
[24] C. Bonifazi, for the Pierre Auger Collaboration, paper 1079, these proceedings.